

Vibronic Transitions in Single Metalloporphyrins

H. J. Lee,^[a] J. H. Lee,^[b] and W. Ho^{*[a]}

Structural and electronic properties of single zinc etioporphyrin molecules adsorbed on Al₂O₃/NiAl(110) were probed by a low-temperature scanning tunneling microscope (STM). Scanning tunneling spectroscopy (STS) revealed progressions of spectral features corresponding to the vibronic states of individual molecules

that depend strongly on the molecular conformations. Vibronic features observed by STS were compared with the results from fluorescence induced by tunneling electrons (tunneling-induced fluorescence, TIF).

Introduction

Electronic and nuclear motions and the interactions between them strongly influence the structure and properties of a molecular system.^[1] Therefore, a complete description of the dynamics of a molecule can be achieved only when the interactions between electronic and nuclear motions are taken into account. The understanding of the coupling between electrons and vibrations in transient molecular species, such as radicals, ions, and excited states, are of particular importance because these play key roles in chemical transformations and in biological processes.

The determination of the expected correlation between the molecular structure and the vibronic coupling requires experimental techniques capable of structural characterization and probing of the vibronic transitions. Single-molecule studies with the scanning tunneling microscope (STM) enable conformation-selective probing of the vibronic coupling, which would otherwise be masked in studies on ensembles of molecules with different adsorption configurations and local environment. We have used a low-temperature STM to probe the vibronic states of single molecules adsorbed on an ultrathin oxide film grown on a metal substrate. The extended lifetime of the transient charged state of the molecule on the oxide film compared to bare metal surface allows observation of vibronic progressions in differential conductance and STM-excited fluorescence spectroscopy.^[2] The different vibronic progressions observed for the same molecule by these two different probing methods highlight the importance of both the initial and final electronic states of a vibronic transition in determining the vibrational modes that strongly couple to the electrons.^[3]

Results and Discussion

The experiments were performed at 19 K by using a home-made STM operated in ultrahigh vacuum.^[4] The NiAl(110) single-crystal surface was prepared by repeated cycles of Ne⁺ sputtering and annealing to 1300 K. Ultrathin (ca. 5 Å thick) aluminum oxide (Al₂O₃) film was grown on the clean NiAl(110) surface by first exposing the surface to 180 L of O₂ at 750 K, followed by subsequent annealing to 1300 K. This procedure resulted in the formation of well-ordered oxide islands,^[5] cover-

ing approximately 50% of the surface. Evaporation of zinc(II) etioporphyrin-I (ZnEtiol) molecules onto this partially oxidized NiAl surface at 19 K led to individually adsorbed molecules (Figure 1).

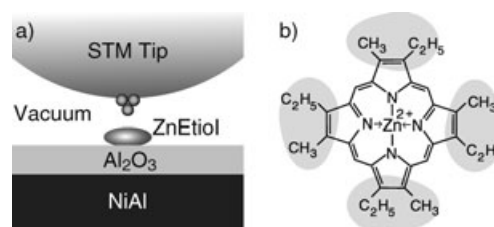


Figure 1. a) Schematic of a double-barrier single-molecule tunneling junction. b) Molecular structure of ZnEtiol. Shaded ovals represent the four lobes in STM images, which appear nonuniform in the case of molecules adsorbed on the oxide (Figure 2).

It was found from STM imaging that the individual ZnEtiol molecules have many different conformations on the oxide surface. This is attributed to the different local environments experienced by the molecules, which arise from the inhomogeneity of the complex oxide film grown on NiAl.^[6–8] The more commonly encountered molecular conformations are shown in Figure 2. Some of these conformations were induced by the STM to reversibly or irreversibly switch to other conformations. The large variety of ZnEtiol conformations is related to the deformation-prone porphyrin macrocycle, which is structurally flexible.^[9] Different electrochemical, vibrational, and optical properties are expected from the various deformations of the porphyrin macrocycle.^[10]

[a] Dr. H. J. Lee, Prof. W. Ho
Department of Physics and Astronomy and Department of Chemistry
University of California, Irvine, California 92697-4575 (USA)
Fax: (+1) 949-824-8125
E-mail: wilsonho@uci.edu

[b] J. H. Lee
Institute of Physics and Applied Physics
Yonsei University, Seoul 120-746 (Korea)

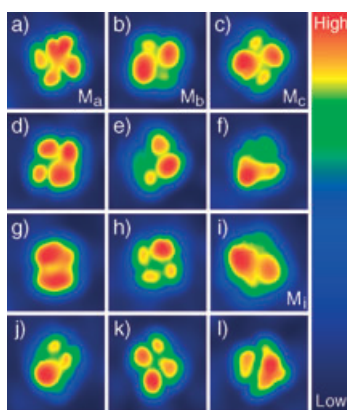


Figure 2. a)–l) $30 \text{ \AA} \times 30 \text{ \AA}$ STM images of some of the more commonly observed conformations of ZnEtIol molecules on $\text{Al}_2\text{O}_3/\text{NiAl}(110)$. All images were obtained at $V_{\text{sample}} = 2.3 \text{ V}$ and $I = 0.25 \text{ nA}$. Some parts of the molecules were easily perturbed by the STM tip, and this is reflected in some of the images. For example, the apparent vertical split and the resulting heart-shaped lobe of the molecule in a) is due to noise in the tunneling current when the tip is above this particular lobe during scanning.

Electronic properties of the different ZnEtIol conformations were probed by scanning tunneling spectroscopy (STS). The dI/dV spectra, which give measures of the local density of states (LDOS),^[11] were obtained via lock-in detection of the first harmonic of the tunneling current with the feedback turned off and applying a modulation voltage to the sample bias. As can be seen in Figure 3, different molecular conformations lead to significantly different electronic properties. The various peaks observed over the molecules are attributed to the unoccupied orbitals of ZnEtIol. For different molecules of the same

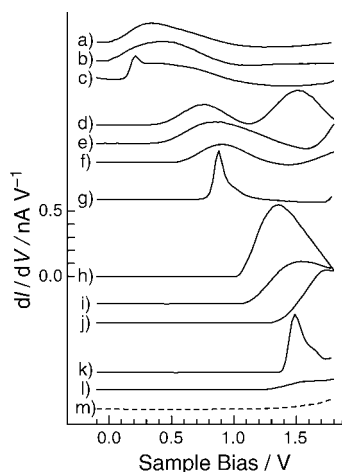


Figure 3. a)–l) dI/dV spectra corresponding to the different conformations of ZnEtIol molecules on $\text{Al}_2\text{O}_3/\text{NiAl}(110)$ as labeled in Figure 2. m) The dI/dV spectrum obtained above a bare aluminum oxide surface is shown as a dashed line. The dI/dV spectra obtained above different lobes of the same molecule were qualitatively similar; therefore, only one representative spectrum for each conformation is shown. The tunneling gap was set at $V_{\text{sample}} = 2.3 \text{ V}$ and $I = 0.25 \text{ nA}$ prior to opening the feedback loop and ramping the sample bias from -0.1 to 1.8 V and back to -0.1 V in 25 mV steps and 300 ms dwell time per step. $10 \text{ mV}_{\text{rms}}$ modulation at 200 Hz was added to the sample bias for lock-in detection. Each spectrum is an average of 10 scans. The spectra are plotted on the same scale and are offset for clarity.

conformation, the dI/dV spectra were qualitatively similar to the representative spectra shown in Figure 3, but the peak energies, widths, and relative intensities varied slightly.

The oxide layer acts as a spacer that reduces the interaction between the metal substrate and the molecule. As a consequence, the lifetime of the transient charged state of the molecule is extended, and this enables detection of vibronic progressions within the molecular electronic resonances. The vibronic progressions were resolved by recording higher resolution dI/dV and d^2I/dV^2 spectra starting at the onsets of molecular electronic resonances for various molecular conformations. The results for the M_a and M_b types of conformations in Figure 2 are shown in Figure 4. The $I-V$ characteristics for M_a and M_b (Figures 4a and 4e) are similar, both showing a smooth rise in conductivity above the Fermi level. The dI/dV spectra for M_a and M_b reveal molecular electronic resonances near the Fermi level (Figures 4b and 4f). On careful examination, subtle corrugations in the broad electronic structures can be discerned, but the exact energy positions of these features

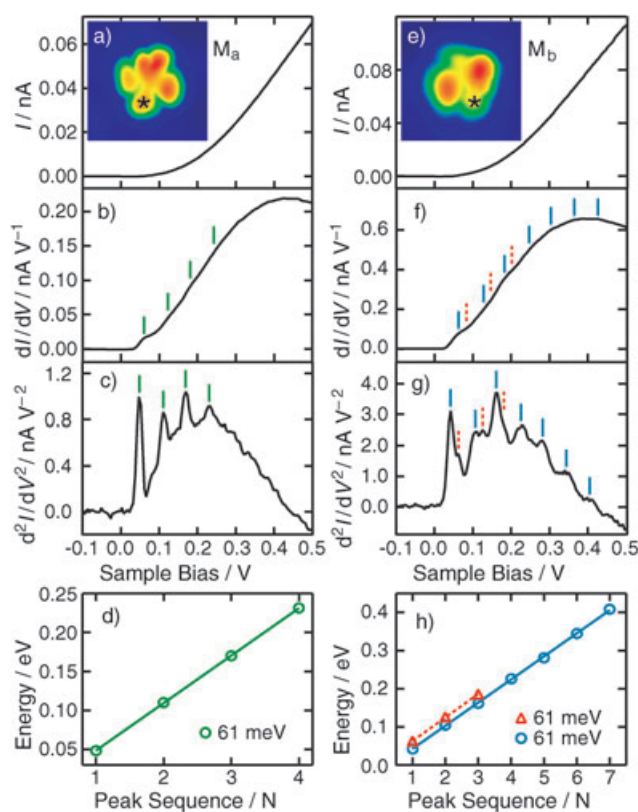


Figure 4. $I-V$ curves (a and e) for the molecular conformations labeled as M_a and M_b in Figure 2, respectively. Corresponding dI/dV spectra (b and f) and d^2I/dV^2 spectra (c and g) were obtained simultaneously via lock-in detection. Tunneling gap was set at $V_{\text{sample}} = 2.3 \text{ V}$, $I = 0.25 \text{ nA}$ for M_a and $V_{\text{sample}} = 2.2 \text{ V}$, $I = 0.25 \text{ nA}$ for M_b . Bias voltage step size of 5 mV and 300 ms dwell time per step were used with $10 \text{ mV}_{\text{rms}}$ bias modulation at 200 Hz . The asterisks in the topographic images indicate the tip positions where the spectra were obtained for each conformation. The spectra are averages of 261 and 120 scans for M_a and M_b , respectively, and each scan is from -0.1 to 0.5 V and back to -0.1 V . Short vertical markers indicate the peak positions in the d^2I/dV^2 spectra and the corresponding energy positions of subtle vibronic features in the dI/dV spectra. Energy positions of the vibronic peaks are plotted in d) and h) together with average peak spacings determined from linear fits.

cannot be determined due to their low intensities. These subtle features are revealed in more detail in the d^2I/dV^2 spectra, which were recorded simultaneously with the $I(V)$ and dI/dV spectra via lock-in detection of the second harmonic of the tunneling current. The d^2I/dV^2 spectrum for the M_a conformation (Figure 4c) shows a series of four readily identifiable peaks (indicated by vertical markers) that are spaced equally in energy. The peak spacing is determined from the linear fit to be 61 ± 1 meV (Figure 4d). In the case of the M_b conformation, there are two separate sequences of equally spaced peaks as indicated by the solid and dashed markers in Figure 4g. Three peaks are identified in the “dashed” series, compared to seven peaks in the “solid” series. The peak spacings for the “dashed” and “solid” series were found from linear fits to be both 61 ± 2 meV (Figure 4h). The “dashed” series is offset higher in energy from the “solid” series by 20 ± 2 meV. Peak positions determined from the d^2I/dV^2 spectra and the corresponding markers are transferred to the dI/dV spectra. Since vibronic states correspond to peaks in the dI/dV spectra, the markers identifying peaks in d^2I/dV^2 are shifted uniformly so that the first solid marker is aligned with the most discernible peak in the dI/dV spectra, as shown in Figure 4b and f.

A tunneling mechanism that can give rise to progressions of features in the dI/dV and d^2I/dV^2 spectra is schematically described in Figures 5a and 5b. First, an electron from the tip tunnels onto an unoccupied ZnEtIol electronic level, forming an anionic state $M1^-$ from the neutral molecular state M (Figure 5a). Excitation of molecular vibrations is allowed when the tunneling electrons have energies that are higher than the energy of $M1^-$ in its ground vibrational state. Resonant tunneling occurs when the electron energy matches the energies of different vibronic states of the transient $M1^-$, and we expect to observe a series of peaks in the dI/dV spectra. $M1^-$ can vibrationally relax (indicated by the short black arrow in Figure 5b) before the electron tunnels through the oxide into the NiAl substrate. The extent of this relaxation will be determined by the competition between the vibrational relaxation rate and the electron tunneling rate out of the anionic molecule into the substrate.^[12] We note that it is possible for the electron to leave the molecule in a vibrationally excited state M^* , where the vibrational energy of the molecule is provided by the electron. The vibrational relaxation time and the electron dwell time in the molecule are much shorter than the time interval between two successive electrons tunneling from the tip onto the molecule, so that the molecule is always in the neutral ground state before the next tunneling electron arrives.^[12]

Within this picture, vibronic states are expected to be manifested as a series of peaks in the dI/dV spectrum. If the peak intensities are low in the dI/dV spectrum, the peak spacing for the dI/dV spectrum can be determined from the peak spacing in the d^2I/dV^2 spectrum. We interpret the equally-spaced peaks in the d^2I/dV^2 spectra for the M_a and M_b molecular conformations as vibronic progressions arising from resonant tunneling into the vibronic states of transient anionic molecules. We exclude the possibility that these features arise from closely spaced ZnEtIol orbitals, based on the fact that a spectrum measured on a lobe of ZnEtIol is expected to be dominated by

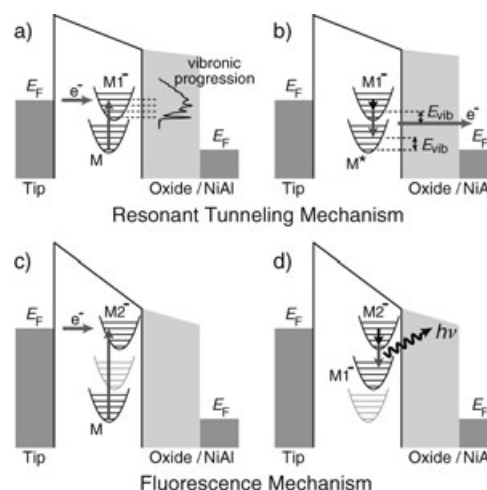


Figure 5. Schematic diagrams comparing the resonant tunneling mechanism (a and b) and STM-excited fluorescence mechanism (c and d) for detecting vibronic features of single molecules supported on an oxide surface (E_F = Fermi level). a) An electron tunnels into an unoccupied molecular electronic level, forming a vibrationally excited singly charged molecule $M1^-$ from the neutral molecule M . Resonant tunneling into the discrete vibronic states of the molecule result in vibronic progressions in the dI/dV and d^2I/dV^2 spectra. b) $M1^-$ vibrationally relaxes, as indicated by the short black arrow. The electron then leaves the molecule (possibly in a vibrationally excited state of the neutral molecule M^* , where the vibrational energy E_{vib} is provided by the electron) and tunnels through the oxide into NiAl. c) An electron tunnels into a higher unoccupied molecular electronic level, forming a charged molecule $M2^-$. d) $M2^-$ vibrationally relaxes (short black arrow), followed by a radiative transition to the lower electronic level $M1^-$ (gray arrow). The last step involves tunneling of the excess electron into the NiAl substrate, which is similar to the process shown in b). The radiative transitions from $M2^-$ to different vibronic states of $M1^-$ result in a progression of features in the light-emission spectra.

a single e_g LUMO, but the number of observed equidistant peaks was four or more.^[2,13] We also exclude the possibility that the observed peaks reflect the final vibrationally excited states of ZnEtIol (M^* in Figure 5b). While the peak spacings measured for various ZnEtIol with the same molecular conformation were the same, the peak positions varied up to several tens of millivolts, depending on the molecule and its local environment. This variation in peak energy directly contradicts the notion that because the observed spacings are the same, a vibrational peak should be observed at an integral number of vibrational quanta from the Fermi level in the case of inelastic electron tunneling spectroscopy (IETS),^[14] and further supports the vibronic origin of the peaks. Furthermore, multiple vibrational excitations have not been resolved in IETS, presumably due to the low cross sections.

The observation of 61 meV peak spacing for both M_a and M_b conformations is interesting in view of the STS results for Cu phthalocyanine (CuPc) on $Al_2O_3/NiAl(110)$, where a vibronic progression with a 61 meV peak spacing was also observed for one of the CuPc conformations.^[15] The occurrence of the same energy spacing in both ZnEtIol and CuPc leads us to assign the 61 meV vibrational mode to the nuclear motions within the overall porphyrin ring that is common to both molecules. This vibrational mode is efficiently coupled to the resonant tunneling mechanism compared to other modes. The two

61 meV progressions, offset by 20 meV from each other in M_b (Figures 4f–4h), are attributed to “progression of progressions”^[11] arising from two vibrational modes with energies of 61 and 20 meV. However, we cannot completely rule out the possibility that this 20 meV offset results from lifting of degeneracy in the electronic states due to Jahn–Teller interaction associated with deformation of the molecule on adsorption. Theoretical analyses are required to arrive at definite conclusions.

Before attempting to assign the vibrational modes corresponding to the observed peak energy spacings, we note that there is a finite voltage drop across the dielectric oxide film. Therefore, the actual energy of the vibrational mode is expected to be smaller than the experimentally measured peak spacing. The voltage drop across the oxide was estimated to be roughly 10–20% of the applied sample bias by using typical tunneling gap distance, oxide thickness, and dielectric constant for alumina.^[16] Taking this voltage drop into account, the 61 and 20 meV peak spacings are in the range of vibrational energies corresponding to the isoindole out-of-plane deformation and isoindole out-of-phase motions, respectively.^[17]

Observation of vibronic features in the d^2I/dV^2 spectra depended strongly on the molecular conformation. At our experimental resolution, we have not been able to detect obvious vibronic features for molecular conformations other than M_a and M_b . Two examples are shown in Figure 6 for the case of M_c and M_i conformations. In the case of M_c , a strong peak at about 0.24 V is observed in dI/dV near the onset of the molecular electronic band together with a lower intensity peak at approximately 0.39 V (Figure 6b). However, we cannot conclu-

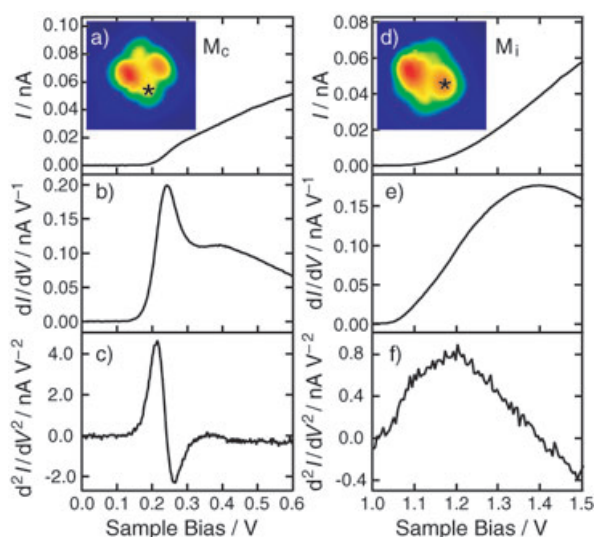


Figure 6. I - V curves (a and d) for the molecular conformations labeled M_c and M_i in Figure 2, respectively. Corresponding dI/dV spectra (b and e) and d^2I/dV^2 spectra (c and f) were obtained simultaneously via lock-in detection. The tunneling gap was set at $V_{\text{sample}} = 2.3$ V, $I = 0.25$ nA for M_c and $V_{\text{sample}} = 2.2$ V, $I = 0.25$ nA for M_i . Bias voltage step sizes of 5 mV and 300 ms dwell time per step were used with 10 mV_{rms} bias modulation at 200 Hz. The asterisks in the topographic images indicate the tip positions where the spectra were obtained for each conformation. The spectra are averages of 10 and 26 scans for M_c and M_i , respectively, from 0.0 to 0.6 V and back to 0.0 V for M_c , and from 1.0 to 1.5 V and back to 1.0 V for M_i .

sively assign these as vibronic features from just two peaks. In the case of M_i , no obvious vibronic features are observed in the spectra (Figures 6e and 6f). It was also found that the presence of oxide spacer between the molecule and NiAl metal substrate is a necessary condition for observation of vibronic features. In the case of ZnEtiol on NiAl metal surface, the lifetime of the transiently charged molecular state is reduced significantly due to higher substrate DOS of the metal. The energy broadening of molecular vibronic states prevents their resolution for molecules adsorbed directly on the metal surface.

Vibronic states of ZnEtiol observed by STS can be compared with the results obtained from fluorescence spectroscopy induced by tunneling electrons or tunneling-induced fluorescence (TIF). In single-molecule TIF, a vibronic progression of 40 ± 2 meV has been reported for the M_c conformation of ZnEtiol on $\text{Al}_2\text{O}_3/\text{NiAl}(110)$.^[2] In contrast, no obvious vibronic feature was observed by STS for the same M_c conformation (Figures 6b and 6c). We also note that the energy of the vibrational mode giving rise to the 61 meV peak spacing for M_a and M_b is larger than 40 meV, even after taking into account the voltage drop across the oxide film. This suggests that different vibronic states are revealed by STS than by TIF. The origin of this difference can be accounted for by examining the mechanisms that give rise to vibronic features in these two different spectroscopic techniques. In the case of TIF, an electron first tunnels into an unoccupied molecular orbital above the LUMO, forming an anionic molecule $M2^-$ (Figure 5c). $M2^-$ can vibrationally relax, followed by a radiative transition to a lower electronic level $M1^-$ (Figure 5d). The last step involves electron tunneling into the NiAl substrate through the oxide, which is similar to the process shown in Figure 5b. The radiative transitions from $M2^-$ to different vibronic states of $M1^-$ result in the observed progression of equally spaced features in the light-emission spectra.^[2] Note that the electronic transitions are not the same for STS versus TIF. Different electronic transitions may involve orbitals of different symmetries and equilibrium internuclear distances, which lead to coupling of electrons to different molecular vibrations. In this regard, a better understanding of electron–vibration coupling in a given adsorbate–substrate system can be obtained by combined studies using both STS and TIF at the molecular level.

Conclusions

In summary, we have studied the effects of the local environment and molecular conformations on electron–vibration coupling using the high spatial resolution of the STM. This local probe allows systematic characterization of different molecular conformations, which cannot be achieved by ensemble-average techniques. Comparison of the STS and TIF results for the same ZnEtiol conformation reveals the different vibronic states that are observed for the two probing methods. Our results highlight the involvement of both the initial and final molecular states in the vibronic transitions, as the symmetry and the equilibrium internuclear distances of these states will deter-

mine which molecular vibrations will have the dominant couplings to the electrons.

Acknowledgments

We thank X. Chen, G. V. Nazin, X. H. Qiu, and S. W. Wu for discussions. This material is based upon work supported by the Chemical Science, Geo- and Bioscience Division, Office of Science, U.S. Department of Energy (grant DE-FG03-01ER15157). Additional support to J.H.L. by the Korean Research Foundation is gratefully acknowledged.

Keywords: electronic structure · fluorescence spectroscopy · scanning probe microscopy · single-molecule studies · vibrational spectroscopy

- [1] G. Herzberg, *Molecular Spectra and Molecular Structure. III. Electronic Spectra and Electronic Structure of Polyatomic Molecules*, Van Nostrand Reinhold, New York, 1966.
- [2] X. H. Qiu, G. V. Nazin, W. Ho, *Science* **2003**, 299, 542.
- [3] The Franck–Condon principle implies that the strongest transition occurs between vibrational states of the initial and final electronic states that have the greatest wavefunction overlap.
- [4] The STM is a variation of that described in B. C. Stipe, M. A. Rezaei, W. Ho, *Rev. Sci. Instrum.* **1999**, 70, 137.
- [5] R. M. Jaeger, H. Kuhlenbeck, H.-J. Freund, M. Wuttig, W. Hoffmann, R. Franchy, H. Ibach, *Surf. Sci.* **1991**, 259, 235.
- [6] M. Baumer, H.-J. Freund, *Prog. Surf. Sci.* **1999**, 61, 127.
- [7] M. Kulawik, N. Nilius, H.-P. Rust, H.-J. Freund, *Phys. Rev. Lett.* **2003**, 91, 256101.
- [8] A. Stierle, F. Renner, R. Streitel, H. Dosch, W. Drube, B. C. Cowie, *Science* **2004**, 303, 1652.
- [9] H. M. Marques, K. L. Brown, *Coordin. Chem. Rev.* **2002**, 225, 123.
- [10] J. A. Shelnett, X.-Z. Song, J.-G. Ma, S.-L. Jia, W. Jentzen, C. J. Medforth, *Chem. Soc. Rev.* **1998**, 27, 31.
- [11] J. Tersoff, D. R. Hamann, *Phys. Rev. Lett.* **1983**, 50, 1998.
- [12] Vibrational relaxation time and the electron dwell time in the molecule adsorbed on a thin oxide film are typically of the order of picoseconds, while the average time interval between two tunneling electrons is on the order of fraction of a nanosecond.
- [13] A. M. Schaffer, M. Gouterman, E. R. Davidson, *Theor. Chim. Acta* **1973**, 30, 9.
- [14] a) B. C. Stipe, M. A. Rezaei, W. Ho, *Science* **1998**, 280, 1732; b) W. Ho, *J. Chem. Phys.* **2002**, 117, 11 033.
- [15] X. H. Qiu, G. V. Nazin, W. Ho, *Phys. Rev. Lett.* **2004**, 92, 206102.
- [16] Only a rough estimate is possible due to uncertainties in the tip height above the surface as well as local dielectric properties of the oxide film.
- [17] B. J. Palys, D. M. W. van den Ham, W. Briels, D. Feil, *J. Raman Spectrosc.* **1995**, 26, 63.

Received: December 13, 2004